Journal of physics. Condensed matter. 2013, vol. 25, no. 11, art. no. 115404. http://dx.doi.org/10.1088/0953-8984/25/11/115404

Vibrational properties and the stability of the $KCuF_3$ phases

Dominik Legut[1] **and Urszula D. Wdowik**[2]

[1] Nanotechnology Centre, VSB-Technical University of Ostrava, 17. listopadu 15, CZ-708 33 Ostrava, Czech Republic

[2] Institute of Technology, Pedagogical University, ul. Podchorazych 2, PL-30-084 Cracow, Poland

E-mail: dominik.legut@vsb.cz

Abstract. We report theoretical investigations of the lattice dynamics of $KCuF_3$. Our calculations are based on the generalized gradient approximation and parametrization of Pedrew-Burke-Ernzerhof (PBE) to the density functional theory corrected for on-site Coulomb interaction (GGA+U). Vibrations of the $KCuF_3$ lattice are studied within the harmonic approximation. Energetic stability of tetragonal and orthorhombic polymorphic structures of $KCuF_3$ is analyzed. Our results show that the orthorhombic polymorph is energetically not preferred. The Raman and infrared-active phonon modes in two distinct tetragonal polymorphs of $KCuF_3$ are discussed with respect to the available experimental data. A detailed examination of the phonon densities of states in both tetragonal polymorphic structures of $KCuF_3$ is provided together with discussion on similarities and differences between the vibrational dynamics of two distinct tetragonal lattices of the $KCuF_3$ system.

PACS numbers: 63.20.-e, 63.20.D-,75.25.-j

Submitted to: *J. Phys.: Condens. Matter*

1. Introduction

$KCuF_3$ is a well-know example of a system which exhibits one-dimensional (1D) magnetic behavior within a three-dimensional magnetic ion sublattice [1]. It was shown by various experimental and theoretical studies that the quasi-1D properties of $KCuF_3$ are due to an interplay between the exchange interaction and orbital-ordering effects associated with the cooperative Jahn-Teller distortions of CuF_6 octahedra [2]-[28].

There are two different tetragonal crystal polymorphs of $KCuF_3$ that are stable in a wide temperature range [1]-[6], i.e. an *a*-type structure (space group $I4/mcm$, No. 140) and a *d*-type structure (space group $P4/mbm$, No. 127). They show slightly different arrangements of the fluorine ions (see figure 1). In the $I4/mcm$ polymorphic phase the K and Cu cations occupy ($4a$) and ($4d$) sites, respectively. There are two crystallographically non-equivalent positions of the fluorine ions. The F_1^- ions are located at ($4b$) sites, whereas F_2^- ions take positions at ($8h$) sites with $x = 0.2276$ [2]. In the $P4/mbm$ structure the K and Cu cations occupy ($2b$) and ($2d$) sites, while F_1^- and F_2^- ions are respectively at the ($2c$) and ($4g$) Wyckoff positions with $x = 0.2273$ [3]. Both polymorphs usually coexist in a given sample [4] and both exhibit *A*-type antiferromagnetic ordering with spins on the Cu cations confined within the $a - b$ plane, the magnetic propagation vector $\langle 001 \rangle$, and a small magnetic moment of about! 0.5 μ_B per each Cu cation cite Hutchings69. These polymorphs also exhibit distinct Néel temperatures, with $T_N = 39$ K and $T_N = 23$ K for the *a*-type and *d*-type structures [5, 6], respectively. Although these two tetragonal polymorphs are commonly accepted, there still exists some ambiguity about the crystal structure of $KCuF_3$. A lower symmetry than tetragonal one reported in early experiments [1]-[6] has been already suggested by Ueda *et al* [7] to explain a weak splitting of two E_g modes observed at 10 K in the polarized Raman spectra. The recent Raman and x-ray scattering experiments [8] as well as optical and infrared measurements [9, 10] also report some possible changes in the symmetry of $KCuF_3$. A reduction in the crystal symmetry from tetragonal to orthorhombic with the space group $P2_12_12_1$ (No. 19), originally proposed by Hidaka *et al* [11], is ascribed solely to! the cooperative displacement of the F^- ions that shift their positions from the midpoint between nearest-neighbor Cu^{2+} ions. On one hand, the static orthorhombic distortions allowed for better explanation of some features of the Raman [7] and electron paramagnetic resonance (EPR) spectra [12], but on the other hand, they were inconsistent with the results of the nuclear quadrupole resonance (NQR) [13], antiferromagnetic resonance [14, 15], electron spin resonance [16] and high-resolution neutron diffraction [17] measurements. Furthermore, the theoretical investigations performed by Binggeli *et al* [18] do not support assumption about the symmetry lowering of the $KCuF_3$ crystal.

The magnetic couplings in $KCuF_3$ are highly anisotropic with strong antiferromagnetic exchange interactions between adjacent Cu^{2+} ions along the *c*-axis and weak ferromagnetic exchange coupling between Cu^{2+} nearest-neighbors ions within the tetragonal $a - b$ plane [19]-[23]. The experimentally determined ratio between the interchain

and intrachain coupling constants $J_{a-b}/J_c \sim -0.01$ with $J_c = 190$ K [21] suggests that above the respective magnetic ordering temperature, the $KCuF_3$ systems are good realizations of the one-dimensional (1D) antiferromagnetic nearest-neighbor Heisenberg model, while below T_N the long-range three-dimensional (3D) antiferromagnetic ordering is maintained.

Most of the experimental and theoretical research on the $KCuF_3$ system has been focused on its *a*-type polymorph with the $I4/mcm$ structure [24]-[28]. In this work we consider predominantly tetragonal structures of $KCuF_3$ and analyze their energetic stabilities as well as vibrational properties. Results of the present studies for the *a*-type polymorph with $I4/mcm$ structure are discussed in the light of the available experimental data, whereas we make a prediction about the lattice dynamics of the *d*-type polymorph with $P4/mbm$ structure. We extend our description of the $KCuF_3$ system by providing additional information on the structural stability of a controversial orthorhombic phase of $KCuF_3$ which we gain from phonons calculated within a plane-wave pseudopotential formulation of density functional theory (DFT).

2. Methodology

In this work, we adopted the VASP package [29], a plane-wave pseudopotential DFT code, to perform spin-polarized calculations on the $KCuF_3$ system. Projector-augmented wave pseudopotentials (PAWs) were used for K, Cu, and F atoms with the valence configurations of ($3p^6 4s^1$), ($3d^1 04s^1$), and ($2s^2 2p^5$), respectively. Gradient corrected exchange-correlation functionals parametrized by Perdew-Burke-Ernzerhof (PBE) [30] and the plane wave cutoff of 520 eV were used. Electron correlation beyond the generalized gradient approximation (GGA) was taken into account within the framework of GGA+U and the approach proposed by Dudarev *et al* [31]. Calculations were carried out with the Coulomb repulsion $U_{\text{eff}} = U - J = 6.1$ eV and the local exchange interaction $J = 0.9$ eV applied for the *d* electrons of Cu atoms. We note that the Coulomb and exchange parameters employed in the present work are similar to those used by Liechtenstein *et al* [32] in their calculations of the *d*-type structure of $KCuF_3$ ($U = 7.5$ eV and $J = 0.9$ eV) as well those applied by Caciuffo *et al* [25] or Binggeli *et al* [18] for the theoretical description of the *a*-type polymorph. Our GGA+U calculations result in the energy gaps of 2.67 eV and 2.06 eV for the *a*-type ($I4/mcm$) and *d*-type ($P4/mbm$) polymorphs, respectively, and correspond to those obtained by other groups for the *a*-type (2.47 eV [25]) and *d*-type (2.0 eV [32]) structures. We mention that the magnitude of the band gap in $KCuF_3$ predicted by various *ab initio* techniques [27], including recently developed computational scheme based on combination of DFT in the GGA approximation and the dynamical mean-field theory (GGA+DMFT) [33], lies in the range of 1.5–3.5 eV [28].

The spin magnetic moment (m_S) on the Cu cation calculated for each structural polymorph of $KCuF_3$ amounts to 0.80 μ_B. It remains significantly overestimated with respect to the experimental value of 0.49(7) μ_B measured at 4 K [5]. We note, however,

that the calculated m_S depends on the applied U_{eff}. Generally, increasing U_{eff} within the GGA/PBE+U leads to a more localized magnetization density compared to GGA/PBE, and thus increases the local magnetic moments. One is able to obtain experimental value of m_S at the GGA/PBE limit, i.e. for $U_{\text{eff}} = 0$ eV. Similar enhancement of the calculated magnetization ($m_S = 0.90 - 0.98\,\mu_B$) was reported by Binggeli *et al* [18]. Also, no improvement of the predicted magnetization was achieved in the recent investigations employing standard (B3LYP) and two range-separated hybrid (HSE and LC-ωPBE) exchange-correlation functionals [34]. The latter still considerably overestimate the experimental spin magnetic moment on the Cu cation, predicting $m_S = 0.81 - 0.84\,\mu_B$. The small value of the experimental m_S in $KCuF_3$ was suggested to originate from the zero-point fluctuations in the spin direction that lower the expectation value of m_S [18]. Indeed, such fluctuations may be large in $KCuF_3$ and can arise from the quasi-1D features of its magnetic structure.

Geometry optimizations of both tetragonal polymorphs were performed for the A-type antiferromagnetic (A-AF) supercells containing 20 atoms. Each supercell was sampled with the k-point mesh of $4\times4\times3$ generated according to the scheme proposed by Monkhorst and Pack. The convergence criteria for the total energies and forces in each supercell were set to 10^{-7} eV and 10^{-5} eV/Å, respectively. To obtain phonons within the direct method approach [35] we used the optimized structures to construct the A-AF supercells that contained 160 and 80 atoms for the $I4/mcm$ and $P4/mbm$ lattices, respectively. These supercells were sampled with the $2 \times 2 \times 2$ k-point mesh. The non-vanishing Hellmann-Feynman forces acting on the atoms in the A-AF supercells were generated by displacing crystallographically nonequivalent K, Cu, and F atoms from their equilibrium positions with the amplitude of 0.03 Å and employing both positive and negati! ve displacements to minimize systematic error. Hence, the total number of calculated displacements amounted to 16 for each tetragonal polymorph. Similar procedure was applied to the orthorhombic phase proposed by Hidaka *et al* [11]. The latter structure is characterized by 10 crystallographically non-equivalent sites building up 40-atom cell of $P2_12_12_1$ symmetry. The number of required displacements to calculate phonons for such a supercell equals to 60.

The transverse components of the infrared active optical phonons (TO modes) were calculated directly from the diagonalization of the system dynamical matrix, while the longitudinal components (LO modes) were obtained by introducing the non-analytical term [36] into the dynamical matrix of the system. In general, this term depends on the Born effective charge tensor $\mathbf{Z}^*$ and the high-frequency dielectric constant ε_∞. The Z^* tensor was calculated using the linear response method [37], while the ε_∞ tensor has been estimated from the real part of the calculated dielectric function.

3. Results and Discussion

Results of structural relaxations performed for the $I4/mcm$, $P4/mbm$, and $P2_12_12_1$ polymorphic structures of $KCuF_3$ are summarized and compared to the experimental

data [2, 3, 11] in Table 1 and Table 2. In general, the calculated lattice constants remain about 2% higher than those measured in experiments. This effect results from a usage of GGA-PBE approximation for the exchange-correlation term. The most pronounced differences between the experimental and theoretical results are found in the positions of the F_1^- and F_2^- ions of the orthorhombic structure, while the position of the remaining non-equivalent F^-, Cu^{2+}, and K^+ ions are very close to those reported by Hidaka *et al* [11]. The calculated shifts of F_1^- and F_2^- ions from the Cu-Cu bonding lines are almost one order of magnitude smaller compared to those given in [11]. These may indicate that displacements of the latter ions deduced from x-ray diffraction [**?**] could be of *dynamic* character and thermally driven, as suggested by Eremin *et al* [16] and Lee *et al* [8]. Moreover, the recent electron spin resonance data have been successfully explained within the tetragonal symmetry and by taking into consideration a dynamical Dzyaloshinsky-Moriya interaction related to the oscillations of the fluorine ions perpendicular to the c-axis of the system [16].

An analysis of the ground state energies of the $KCuF_3$ polymorphic structures shows that the $I4/mcm$ polymorph is lower in energy than $P2_12_12_1$ and $P4/mbm$ ones by 0.8 and 1.5 meV per formula unit (f.u.), respectively. The energetic sequence in the ground state, $E_0(I4/mcm) < E_0(P2_12_12_1) < E_0(P4/mbm)$, becomes somewhat different when the zero-point energy motion obtained from the phonon calculations is taken into account. It occurs that the free energy of phonons (E_{vib}) pushes up the energy $E = E_0 + E_{vib}$ of the $P2_12_12_1$ structure above the energy E of the $P4/mbm$ structure. Finally, the following sequence of the energetic stability is maintained $E(I4/mcm) < E(P4/mbm) < E(P2_12_12_1)$. It holds up below the room temperature, as indicated in figure 2. At zero temperature, the difference between the energies of the most stable $I4/mcm$ polymorph and $P4/mbm$ is as small as ∼4 meV/f.u., while the energy difference between $I4/mcm$ and! $P2_12_12_1$ structures amounts to ∼7 meV/f.u.. Both energy differences increase with increasing temperature, provided the harmonic approximation applies.

According to the calculated energetic stability of the $KCuF_3$ phases, we analyze and compare vibrational properties of two tetragonal polymorphs. At the Γ-point the phonons of the $I4/mbm$ and $P4/mcm$ polymorphic structures can be classified according to the irreducible representations of the respective point groups D_{4h}^{18} and D_{4h}^{5} as follows:

$$I4/mcm: \; 6E_u^{(2)} + 4A_{2u} + 3E_g^{(2)} + A_{1g} + B_{1g} + 2B_{2g} + 2A_{2g} + 2B_{1u}$$
$$P4/mbm: 8E_u^{(2)} + 4A_{2u} + E_g^{(2)} + A_{1g} + B_{1g} + B_{2g} + A_{2g} + A_{1u} + 3B_{1u}\,.$$

The modes E_u and A_{2u} are infrared (IR) active, while E_g, A_{1g}, B_{1g}, and B_{2g} are Raman active. The E_u and E_g modes remain doubly degenerate. The A_{2u}+$E_u^{(2)}$ phonons constitute lattice translational modes. Remaining modes, namely, A_{2g}, B_{1u}, and the A_{1u} mode in the $P4/mbm$ polymorph are optically inactive (silent).

In the Raman active modes the Cu ions are at rest as they are located at inversion centers. No contribution to the Raman modes in the $P4/mbm$ structure comes neither from the F_1^- nor K^+ sublattices. Vibrations of the K^+ ions perpendicular to the c-axis in

the $I4/mcm$ structure give rise to the E_g modes. These modes involve also movements of the F_1^- and F_2^- sublattices perpendicular and parallel to the c-axis, respectively. The modes A_{1g}, B_{1g}, and B_{2g} in both polymorphs arise from the F_2^- ions vibrating perpendicular to the c-axis. In addition, the B_{2g} mode in the $I4/mcm$ polymorph contains vibrations of the F_1^- sublattice along the c-axis.

Figure 4 compares the frequencies of Raman modes calculated for the $I4/mcm$ and $P4/mbm$ structural polymorphs of $KCuF_3$ with the experimental frequencies measured at 10 K by Ueda *et al* [7]. We notice that A_{1g} and B_{1g} modes in both polymorphs show very similar frequencies. Essential differences are found for the E_g and B_{2g} phonons resonating at different frequencies in each polymorph. The E_g mode at $\sim$200 cm^{-1} which corresponds to a motion of the F_2^- ions along the c-axis in the $P4/mbm$ structure appears nearly in-between the lowest and the highest-frequency E_g modes in the $I4/mcm$ structure, the latter being due to sharing vibrations of both fluorine sublattices. The mode of B_{2g} symmetry, corresponding in the $P4/mbm$ structure to the stretching vibrations of the F_2^- sublattice, lies $\sim$40 cm^{-1} below the highest-frequency B_{2g} mode of the $I4/mcm$ structure. The latter mode! involves not only displacements of the F_2^- but also vibrations of the F_1^- sublattice. In principle, above features could be used to distinguish one polymorphic structure from another in a given sample of $KCuF_3$.

In both polymorphic structures of $KCuF_3$, the IR-active A_{2u} and E_u phonons correspond to oscillations of the dipole moment parallel and perpendicular to the c-axis, respectively. Frequencies of these modes are displayed in figure 5. The frequencies of the LO modes were obtained using the calculated tensors $\mathbf{Z}^*$ and ε listed in Table 3. The components of the ε tensor parallel (ε_{33}) and perpendicular (ε_{11}) to the c-axis were estimated from the $E \to 0$ limit of the real part of dielectric function shown in figure 3. We compare results of our calculations to the experimental TO frequencies measured at 12 K by Deisenhofer *et al* [10]. The reflectivity and dielectric loss spectra reveal a two-peak structure of the E_u mode at $\sim$200 cm^{-1} which vanishes above 150 K, i.e. far above the respective Néel temperatures of both p! olymorphs. This feature was assigned to a splitting of the doubly degenerated E_u mode. The IR phonon of A_{2u} symmetry at $\sim$250 cm^{-1} also exhibits some anomalous behavior below 150 K, which was related to the multiphonon processes [10]. Such a deviation is not observed neither for the calculated E_u nor A_{2u} mode. Results of our calculations indicate that the modes of A_{2u} symmetry as well as the highest-frequency E_u mode appear in both structural polymorphs of $KCuF_3$ at very similar frequencies. Below $\sim$260 cm^{-1}, a small shift between theoretical and experimental frequencies of the E_u modes in the $I4/mcm$ structure is observed. Nevertheless, the IR spectrum of the $P4/mbm$ polymorph differs from the respective spectrum of the $I4/mcm$ polymorph since it contains additional E_u vibrational mode at $\sim$95 cm^{-1}. Although, the frequency of this mode is close to the frequency of an additional mode at $\sim$107 cm^{-1}, which develops in ! the experimental IR spectra below 40 K, it is unlikely to arise from the $P4/mbm$ polymorph as it remains visible for both polarizations (parallel and perpendicular to the the c-axis). It was suggested, that this low-frequency mode can be either magnetic in its origin or it may correspond to

a phonon mode of the orthorhombic structure. On one hand, a possible orthorhombic structure [11] would show three IR-active modes of B_1 and B_3 symmetries in the very close vicinity of the mode at 107 cm^{-1}, but on the other hand, its IR-spectrum would exhibit much finer structure than that reported in [10]. In general, the total number of the IR-active phonons of B_1, B_2, and B_3 symmetries in the orthorhombic phase with the $P2_12_12_1$ space group amounts to 90. Our calculations showed, however, that such a structure is unfavorable as far as the energetic stability is concerned. Therefore, it is more plausible that this additional low-frequency mode appearing in the IR spectra of KCuF! $_3$ measured at low temperatures is rather of magnetic nature.

We used the calculated LO-TO splitting of the IR-active modes to estimate the static dielectric tensor ε_0 of the $KCuF_3$ system. The ε_0 can be factored into contribution arising from purely electronic screening ε_∞ and the IR-active phonon modes as follows [38]:

$$\varepsilon_0 = \varepsilon_\infty + \varepsilon_\infty \sum_i \left(\frac{\omega_{LO,i}^2}{\omega_{TO,i}^2} - 1 \right) , \quad (1)$$

where $\omega_{TO,i}$ and $\omega_{LO,i}$ are the TO and LO frequencies of the IR-active modes. The components perpendicular ($\varepsilon_0^\perp$) and parallel ($\varepsilon_0^\parallel$) to the c-axis are following: $\varepsilon_0^\perp(I4/mcm) = 5.82$, $\varepsilon_0^\perp(P4/mbm) = 6.09$, $\varepsilon_0^\parallel(I4/mcm) = 6.13$, and $\varepsilon_0^\parallel(P4/mbm) = 6.52$. Our results indicate that both components of the ε_0 tensor of the $P4/mbm$ structure are slightly higher than the respective components of the $I4/mcm$ structure.

Additional information on the dynamics of the $KCuF_3$ polymorphic phases considered in the present work can be gained from the calculated phonon densities of states (DOS). The total densities of the phonon states for both tetragonal structures of KCuF3 are displayed in figure 6. The phonon DOS of each polymorph spans the spectral range from 0 to 70 meV. One notices that these two phonon spectra show some differences, especially in the energy range of 18-33 meV (145-266 cm^{-1}). To find out about the source of the observed differences, it is advantageous to separate the phonon DOS into contributions from vibrations of particular sublattices constituting the $KCuF_3$ system. Such contributions, i.e. partial densities of states (pDOS) calculated for the $I4/mcm$ and $P4/mbm$ polymorphs are also shown in figure 6. Below 25 meV, the phonon spectrum in each polymorph is dominated by the vibrations of the K^+ sublattice. A difference between the dy! namics of the respective K^+ sublattices is rather insignificant. The pDOS of the Cu^{2+} sublattice in each polymorph shows energy distribution in two ranges, i.e. up to 40 meV and above 50 meV. In the highest frequency region, the partial densities of states due to vibrations of the Cu^{2+} ions in the $I4/mcm$ and $P4/mbm$ systems are similar to each other. The differences in the dynamics between these two sublattices are observed in the range of 20-33 meV, where the Cu pDOS in the $P4/mbm$ polymorph exhibits two phonon peaks, not present in the respective pDOS of the $I4/mcm$ polymorph. The phonons resulting from the vibrations of the F^- ions cover the entire spectral range. These are pure fluorine vibrations between 40 and 50 meV, where no contribution to the density of states comes from the cation sublattices. Below

33 meV, the partial densities of states due to the F^- ions arise from the F_1^- sublattices vibrating perpendicular to the c-axis, while the vibrations of the $F_1!^-$ ions along the c-axis dominate at higher energies. The F_2^- sublattice vibrations perpendicular to the c-axis span the entire spectral range, whereas the F_2^- sublattice vibrations parallel to this axis are limited to about 40 meV. Apart many similarities between the dynamics of the F^- sublattices in the $I4/mcm$ and $P4/mbm$ polymorphs we find some differences in the energy range of 20-33 meV and they are also observed in the respective Raman spectra. For example, the E_g mode appearing at ∼25 meV (∼200 cm^{-1}) in the Raman spectrum of the $P4/mbm$ structure remains also well-resolved in the phonon DOS spectrum.

Finally, we used the harmonic approximation and the phonon DOS to obtain the lattice contribution to the heat capacity. Figure 7 shows the temperature evolution of the heat capacity divided by temperature (C/T) for the $I4/mcm$ and $P4/mbm$ polymorphs. The calculated C/T remains in close agreement with the results of the measurements reported by Deisenhofer *et al* [10]. It should be noted that the experimental heat capacity contains also the magnetic contribution, and thus a typical λ-type behavior is expected in the vicinity of the respective Néel temperatures (39 K and 23 K). Nevertheless, the lattice contributions to the heat capacities of the $I4/mcm$ and $P4/mbm$ polymorphs are distinguishable from each other below ∼ 100K, while at higher temperatures they become identical.

4. Summary and conclusions

An analysis of the energetic stability performed for two tetragonal polymorphs of $KCuF_3$ as well as the orthorhombic polymorph with the symmetry proposed by some x-ray diffraction experiments [11] indicates that the orthorhombic polymorph is the least stable phase among those considered in the present work. It was shown that the zero-point energy motion plays a significant role in predicting the energetic stability of the $KCuF_3$ phases. The static displacements of the fluorine ions that lead to the orthorhombic symmetry are calculated to be about one order of magnitude smaller than those reported in the x-ray diffraction studies [11]. This suggest that the symmetry lowering may arise from thermally driven distortion as shown also by the calculated frequencies of the Raman and infrared modes that remain in close agreement with the experimental data determined for the tetragonal symmetry of $KCuF_3$. The splitting of some Raman modes as well as the appearance of additional infrared mode in the vicinity of the Néel temperature, ! as observed in some experiments, require further experimental/theoretical verification. A detailed analysis of the phonon density of states spectra, given in the present work, can be useful for the inelastic neutron scattering investigations that could provide additional information on the vibrational dynamics of the $KCuF_3$ lattice.

Acknowledgments

Interdisciplinary Centre for Mathematical and Computational Modelling (ICM), Warsaw University, Poland and National Center CERIT Scientific Cloud (CERIT-SC), Czech Republic are acknowledged for providing the computer facilities to support part of the present calculations under Grants No. G28-12 and Reg. No. CZ.1.05/3.2.00/08.0144. This work was supported by the Czech-Polish Research Project no. MEB 051015-8069/2010. D. Legut acknowledges a support within the framework of the Nanotechnology Centre - the basis for international cooperation project, Reg. No. CZ.1.07/2.3.00/20.0074 and the IT4Innovations Centre of Excellence project, Reg. No. CZ.1.05/1.1.00/02.0070, both supported by Operational Programme 'Education for competitiveness' funded by Structural Funds of the European Union and state budget of the Czech Republic.

References

[1] Okazaki A and Suemune Y 1961 *J. Phys. Soc. Japan* **16** 671, Okazaki A 1969 *J. Phys. Soc. Japan* **26** 870
[2] Tanaka K, Konishi M, and Marumo F 1979 *Acta Cryst. B* **35** 1303
Tanaka K, Konishi M, and Marumo F 1980 *Acta Cryst. B* **36** 1264
Tanaka K and Marumo M 1980 **Acta Cryst. B 38** 1422
[3] Tsukuda N and Okazaki A 1972 *J. Phys. Soc. Jpn.* **33** 1088
[4] Towler M D, Dovesi R and Saunders V R 1995 *Phys. Rev. B* **52** 10150
[5] Hutchings M T, Samuelsen E J., Shirane G and Hirakawa K 1969 *Phys. Rev.* **188** 919
Hutchings M T, Ikeda H and Milne J M 1979 *J. Phys. C* **12** L739
[6] Buttner R H, Malsen E N and Spadaccini N 1990 *Acta Cryst. B* **46** 131
[7] Ueda T, Sugawara K, Kondo T and Ymada I 1991 Sol. State. Commun. **80** 801
[8] Lee J C T, Yuan S, LaI S, Joe Y II, Gan Y, Smadici S, Finkklestein K, Feng Y, Rusydi A, Goldbart P M, Cooper S L and Abbamonte P 2012 *Nature Phys.* **8** 63
[9] Deisenhofer J, Leonov I, Eremin M V, Kant Ch, Ghigna P, Mayr F, Iglamov V V, Anisimov V I and van der Marel D 2008 *Phys. Rev. Lett.* **101** 157406
[10] Deisenhofer J, Schmidt M, Wang Z, Kant C, Mayr F, Schrettle F, Krug von Nidda H-A, Ghigna P, Tsurkan V and Loidl A 2011 *Ann. Phys.* **523** 645
[11] Hidaka M, Eguchi T and Yamada I 1998 *J. Phys. Soc. Japan* **67** 2488
[12] Yamada I, Fuji H, and Hidaka M 1989 *J. Phys. Condens. Matter.* **1** 3397
Ishii T and Yamada I 1990 *J. Phys. Condens. Matter.* **2** 5771
[13] Mazzoli C, Allodi G, De Renzi R, Guidi G and Ghigna P 2002 *J. Magn. Magn. Mat.* **242** 935
[14] Yamada I and Kato N 1994 *J. Phys. Soc. Jpn.* **63** 289
[15] Li L, Shi Q, Mino M, Yamazaki H, and Yamada I 2005 *J. Phys.: Condens. Matter* **17** 2749
[16] Eremin M V, Zakharov D V, Krug von Nidda H-A, Eremina R M, Shuvaev A, Pimenov A, Ghigna P, Deisenhofer J and Loidl A 2008 *Phys. Rev. Lett.* **101** 147601
[17] Zhou J -S, Alonso J A, Han J T, Fernández-Díaz M T, Cheng J -G, and Goodenough J B 2011 *J. Fluor. Chem.* **132** 1117
[18] Bingelli N and Altarelli M 2004 *Phys. Rev. B* **70** 085117.
[19] Bonner J C and Fisher M E 1964 *Phys. Rev.* **135** 640
[20] Oguchi T 1964 *Phys. Rev.* **133** 1098
[21] Satija S K, Axe J D, Shirane G, Yoshizawa H and Hirakawa K 1980 *Phys. Rev. B* **21** 2001
[22] Iio K, Hyodo H, Nagata K and Yamada I 1978 *J. Phys. Soc. Jpn.* **44** 1393

[23] Kadota S, Yamada I, Yoneyama S and Hirakawa K 1967 *J. Phys. Soc. Jpn.* **23** 751
[24] Chakhalian J, Kiefl R F, Brewer J, Dunsiger S R, Morris G, Eggert S, Affleck I and Yamada I 2004 *J. Magn. Magn. Mat.* **272-276** 979
Chakhalian J, Kiefl R F, Miller R, Dunsiger S R, Morris G, Kreitzman S, MacFarlane W A, Sonier J, Eggert S, Affleck I and Yamada I 2003, *Physica B* **326** 422
[25] Caciuffo R, Paolasini L, Sollier A, Ghigna P, Pavarini E, van den Brink J and Altarelli M 2002 *Phys. Rev. B* **65** 17725
[26] Medvedeva J E, Korotin M A, Anisimov V I and Freeman J A 2002 *Phys. Rev. B* **65** 172413
[27] Pavarini E, Koch E and Lichtenstein A I 2008 *Phys. Rev. Lett.* **101** 266405
[28] Leonov I, Binggeli N, Korotin D, Anisimov V I, Strojić N and Vollhardt D 2008 *Phys. Rev. Lett.* **101** 096405
Leonov I, Korotin D, Binggeli N, Anisimov V I and Vollhardt D 2010 *Phys. Rev. B* **81** 075109
[29] Kresse G and Furthmüller J 1996 *Phys. Rev. B* **54** 11169
Kresse G and Furthmüller J 1996 *J. Comput. Mater. Sci.* **6** 15
[30] Perdew J P Burke K and Ernzerhof M 1996 *Phys. Rev. Lett.* **77** 3865
Perdew J P Burke K and Ernzerhof M 1997 *Phys. Rev. Lett.* **78** 1396
[31] Dudarev S L, Botton G A, Savrasov S Y, Humphreys C J and Sutton A P 1998 *Phys. Rev. B* **57** 1505
[32] Liechtenstein A I, Anisimov V I and Zaanen J 1995 *Phys. Rev. B* **52** R5467
[33] Lechermann F, Georges A, Poteryaev A, Biermann S, Posternak M, Yamasaki A and Andersen O K 2006 *Phys. Rev. B* **74** 125120
[34] Rivero P, Moreira I P R, Scuseria G E, Illas F 2009 *Phys. Rev. B* **79** 245129
[35] Parlinski K, *Software PHONON*, Cracow, Poland (2008)
Parlinski K, Li Z -Q and Kawazoe Y 1997 *Phys. Rev. Lett.* **78** 4063
[36] Pick R M, Cohen M H, Martin R M 1970 *Phys. Rev. B* **1** 910
[37] Gajdos M, Hummer K, Kresse G, Furthmüller J and Bechstedt F 2006 *Phys. Rev. B* **73** 045112
[38] Gonze X and Lee C 1997 *Phys. Rev. B* **55** 10337

Table 1. Calculated (experimental) structural parameters of the $I4/mcm$ and $P4/mbm$ polymorphs of $KCuF_3$. The calculated and experimental bond lengths for the three inequivalent Cu–F bonds are denoted by symbols l, m and s.

Structure	a (Å)	c (Å)	x	
$I4/mcm$	5.9716	7.8989	0.2246	
	(5.863)[a]	(7.847)[a]	(0.2276)[a]	
$P4/mbm$	5.9686	3.9511	0.2247	
	(5.854)[b]	(3.930)[b]	(0.2273)[b]	
Bond lengths (Å)				
	K–Cu	l	m	s
$I4/mcm$	3.58	2.33	1.97	1.90
	(3.53)[a]	(2.26)[a]	(1.96)[a]	(1.89)[a]
$P4/mbm$	3.58	2.32	1.98	1.90
	(3.53)[b]	(2.26)[b]	(1.97)[b]	(1.88)[b]

[a] reference [2]
[b] reference [3]

Table 2. Calculated and experimental [11] structural parameters of the orthorhombic $KCuF_3$ polymorph with $P2_12_12_1$ symmetry. The calculated and experimental bond lengths for the three inequivalent Cu–F bonds are denoted by symbols l, m and s.

	Calc.	Exp.
a (Å)	8.4473	8.270
b (Å)	8.4472	8.270
c (Å)	7.8980	7.841
K_1 ($4a$)	(0.25, 0.25, 0.25)	(0.25, 0.25, 0.25)
K_2 ($4a$)	(0.75, 0.25, 0.25)	(0.75, 0.25, 0.25)
Cu_1 ($4a$)	(0.0, 0.0, 0.0)	(0.0, 0.0, 0.0)
Cu_2 ($4a$)	(0.50, 0.0, 0.0)	(0.5, 0.0, 0.0)
F_1 ($4a$)	(0.0011, 0.0011, 0.25)	(0.0115, 0.0115, 0.25)
F_2 ($4a$)	(-0.0011, -0.0011, 0.75)	(-0.0115, -0.0115, 0.75)
F_3 ($4a$)	(0.2245, 0.0, 0.0)	(0.2267, 0.0, 0.0)
F_4 ($4a$)	(0.0, 0.2755, 0.0)	(0.0, 0.2733, 0.0)
F_5 ($4a$)	(0.0, 0.2245, 0.5006)	(0.0, 0.2267, 0.50)
F_6 ($4a$)	(0.7755, 0.0, 0.0006)	(0.7733, 0.0, 0.0)
Bond lengths (Å)		
K–Cu	3.58	3.52
l	2.33	2.26
m	1.97	1.96
s	1.90	1.87

Table 3. Born effective charges for the $I4/mcm$ (a-type) and $P4/mcm$ (d-type) polymorphs of $KCuF_3$. Dielectric tensor components of the a-type: $\varepsilon_{11} = 2.55$, $\varepsilon_{33} = 2.70$, and d-type: $\varepsilon_{11} = 2.58$, $\varepsilon_{33} = 2.75$. Units of effective charges: e.

	Z_{11}		Z_{33}		Z_{12}	
Atom	a-type	d-type	a-type	d-type	a-type	d-type
K	1.198	1.196	1.182	1.182		0.06
Cu	2.048	2.076	2.332	2.342	0.13	0.15
F_1	-0.742	-0.764	-1.838	-1.868		-0.05
F_2	-1.252	-1.254	-0.838	-0.828	-0.39	-0.40

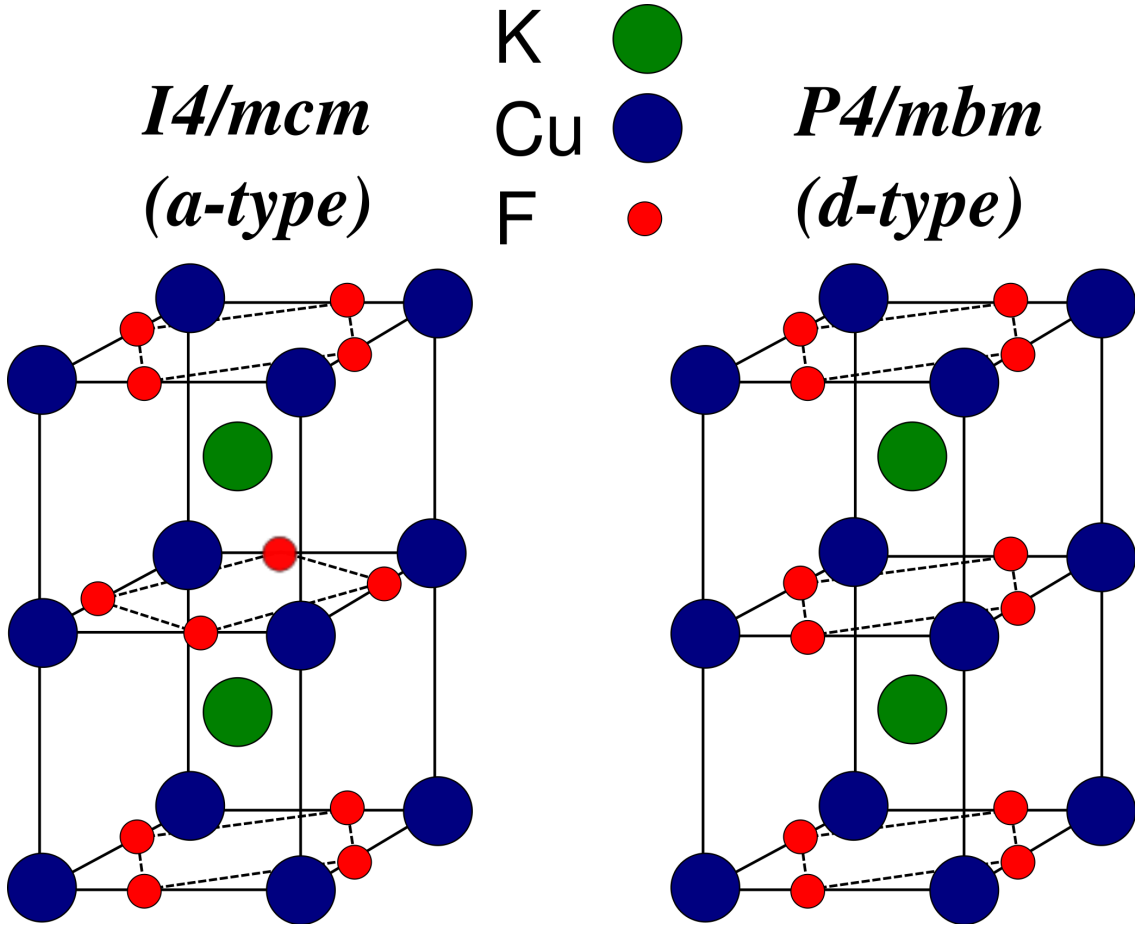

Figure 1. The $I4/mcm$ (a-type) and $P4/mbm$ (d-type) polymorphic structures of $KCuF_3$.

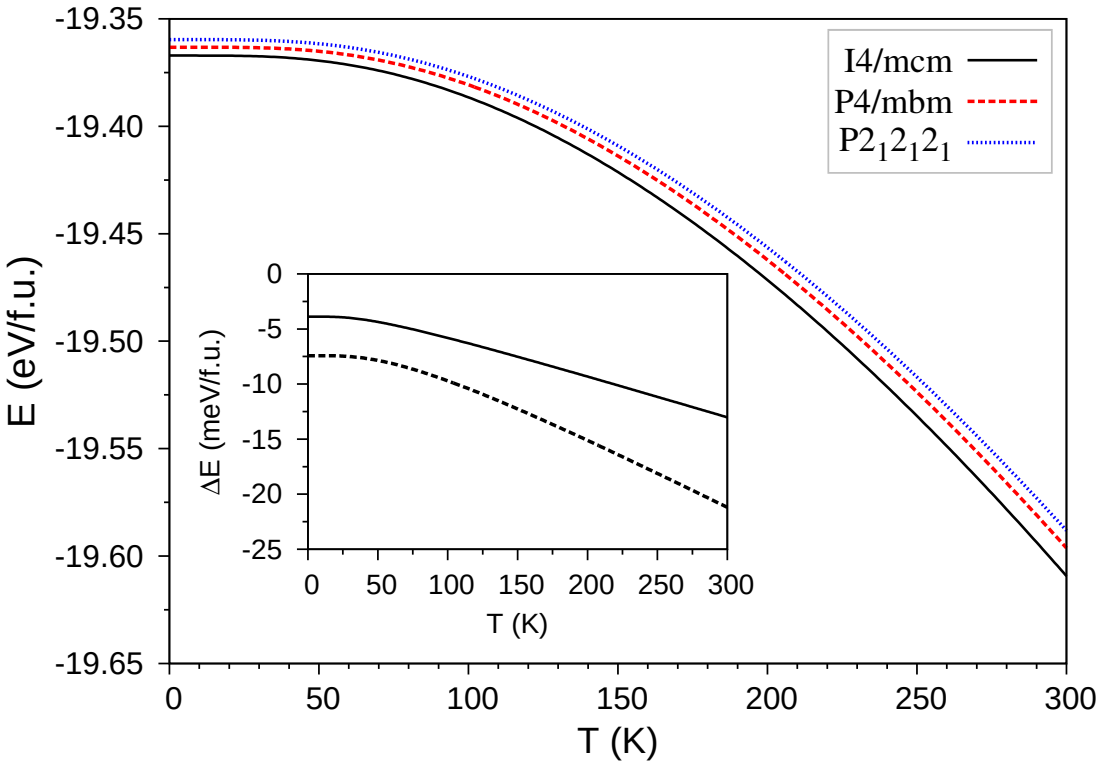

Figure 2. Calculated energy $E = E_0 + E_{vib}$ of the $I4/mcm$ (solid curve), $P4/mbm$ (dashed curve) and orthorhombic $P2_12_12_1$ (dotted curve) structures of $KCuF_3$. (inset) Difference in energies (ΔE) between the $I4/mcm$ and $P4/mbm$ polymorphs (solid curve) and between the $I4/mcm$ and $P2_12_12_1$ ones (dashed curve).

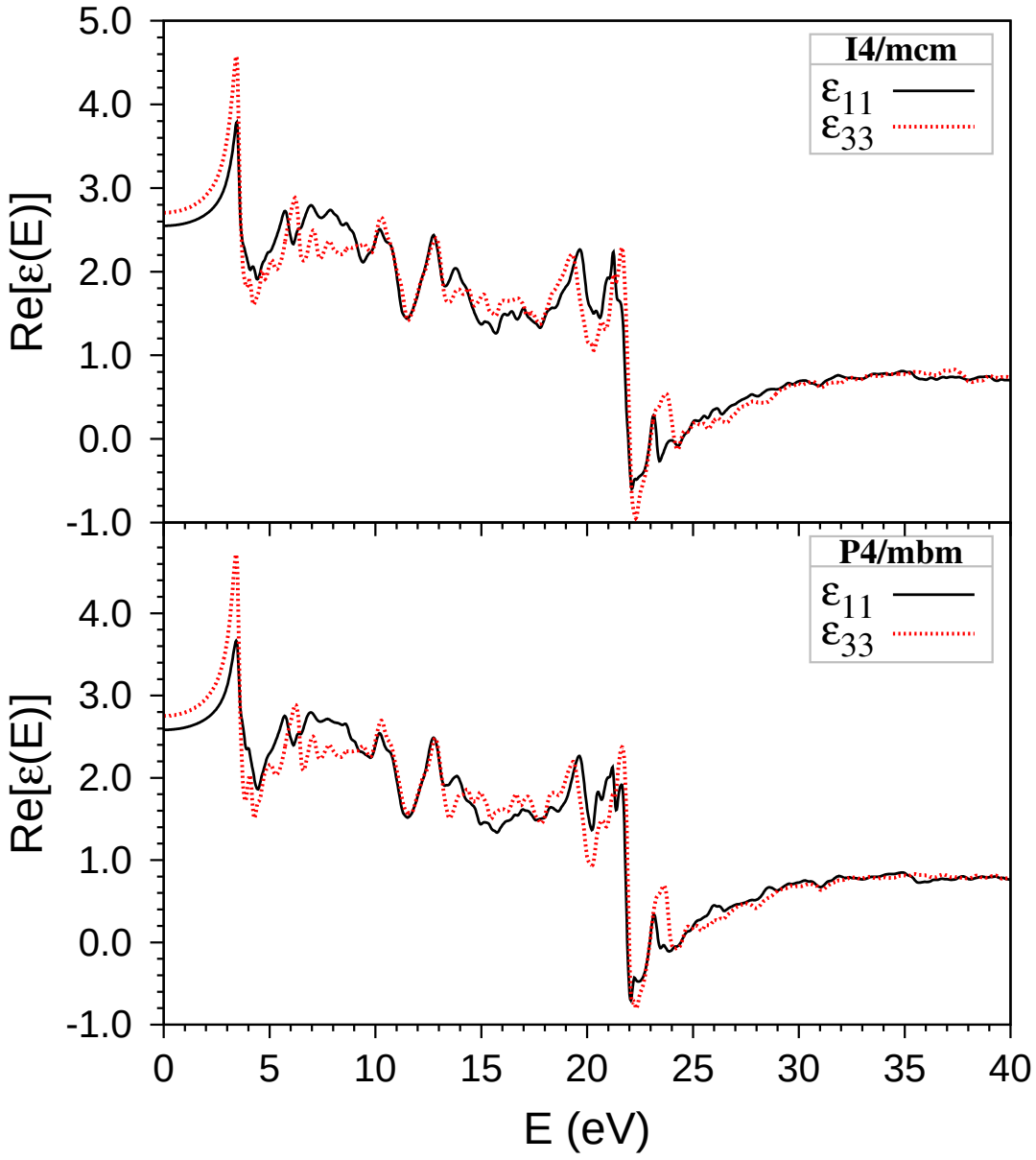

Figure 3. Energy dependence of the real part of dielectric function parallel (ε_{33}) and perpendicular (ε_{11}) to the c-axis for the $I4/mcm$ (a-type) and $P4/mbm$ (d-type) polymorphs of $KCuF_3$.

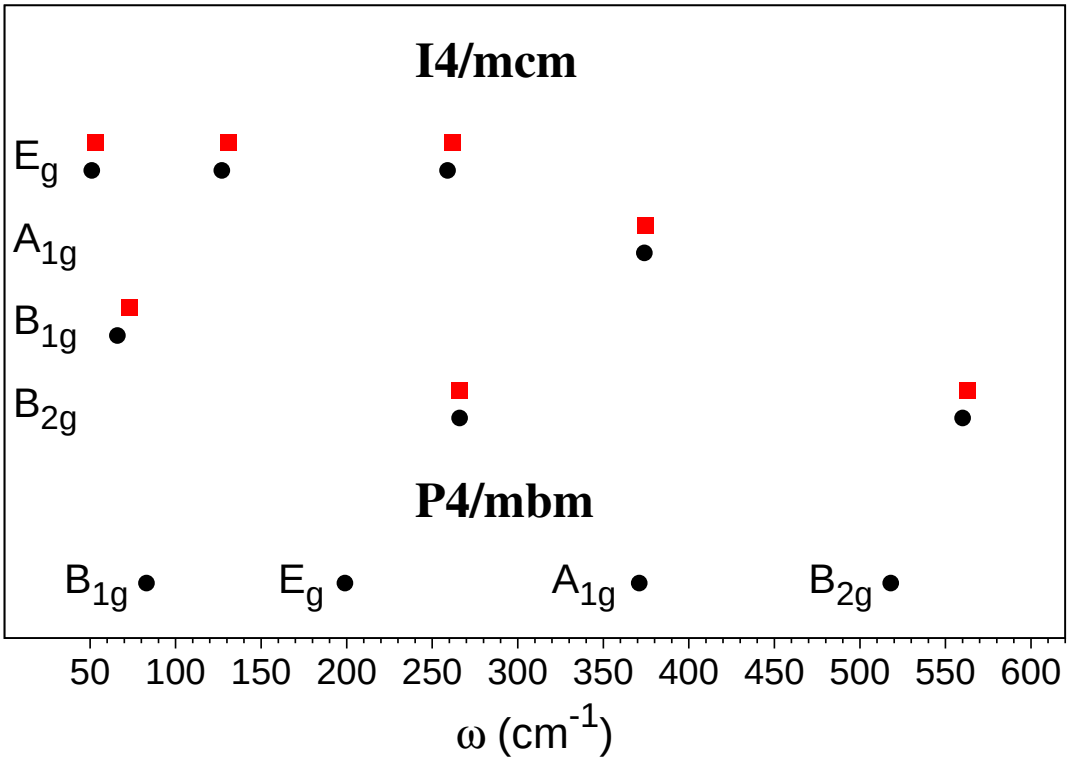

Figure 4. Calculated (circles) and experimental [7] (squares) Raman active modes in the $I4/mcm$ (a-type) and $P4/mbm$ (d-type) polymorphs of $KCuF_3$.

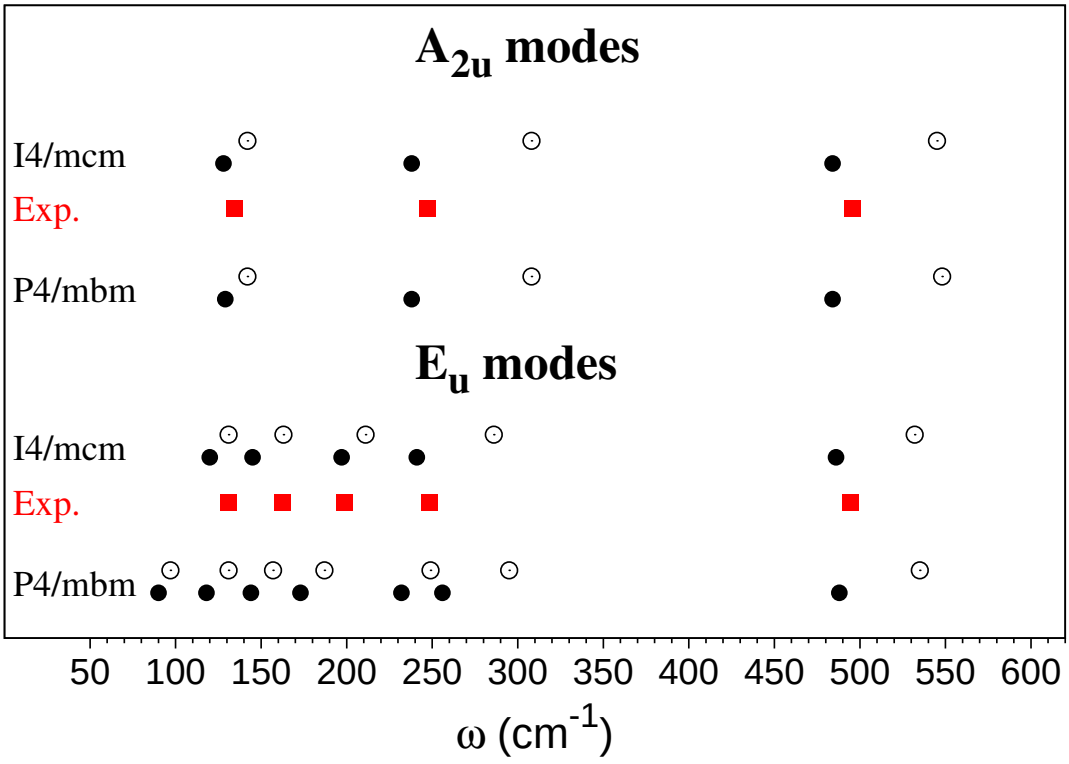

Figure 5. Calculated and experimental [10] IR-active modes in the $I4/mcm$ (a-type) and $P4/mbm$ (d-type) polymorphs of $KCuF_3$. Frequencies of TO and LO modes are indicated by solid and open symbols, respectively. Experimental TO frequencies are denoted by squares.

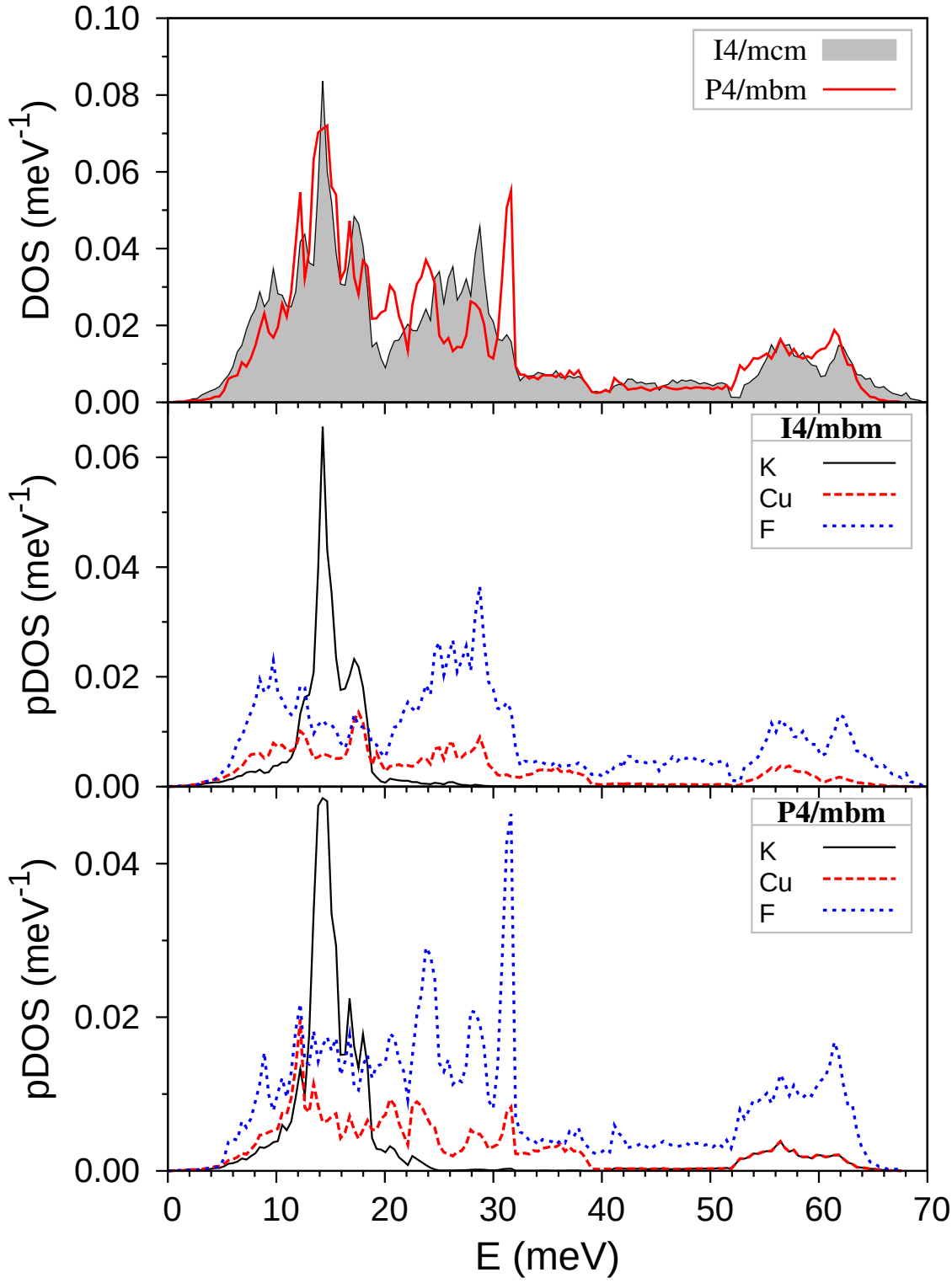

Figure 6. (upper) Total phonon densities of states (DOS) for the $I4/mcm$ (shaded area) and $P4/mbm$ (solid curve) polymorphs of $KCuF_3$. (middle) Partial phonon densities of states (pDOS) due to the K^-, Cu^{2+}, and F^- sublattices in the $I4/mcm$ polymorph. (bottom) Partial phonon densities of states (pDOS) due to the K^-, Cu^{2+}, and F^- sublattices in the $P4/mbm$ polymorph. Partial phonon densities of states for K^-, Cu^{2+}, and F^- sublattices are denoted by solid, dashed and dotted curves, respectively.

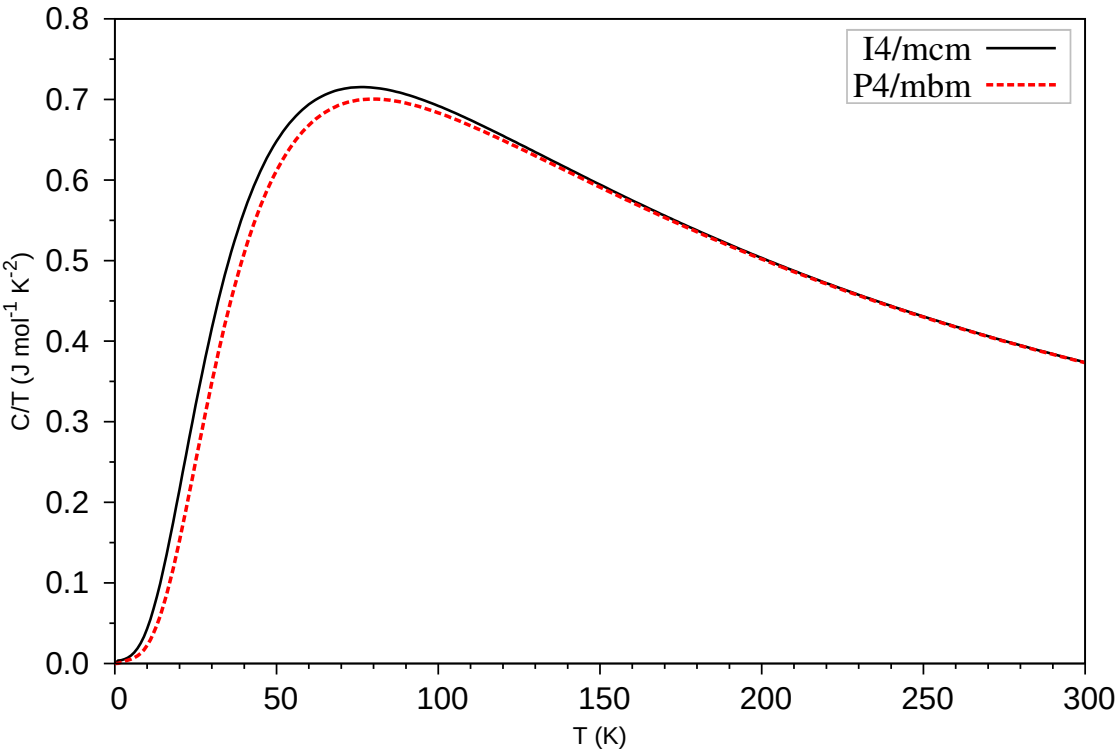

Figure 7. Temperature dependences of C/T calculated for the $I4/mcm$ and $P4/mbm$ polymorphs of $KCuF_3$.